Journal of Molecular Structure 1022 (2012) 25–31

Contents lists available at SciVerse ScienceDirect

Journal of Molecular Structure

journal homepage: www.elsevier.com/locate/molstruc

Synthesis and characterization of three dinuclear complexes of Ag^I with 2,3-bis(2-pyridyl)pyrazine and derivated of trifluoromethyldiketonate ligands

Farzin Marandi [a,*], Afsaneh Marandi [b], Mohammad Ghadermazi [b], Mohammad Rafiee [c], Harald Krautscheid [d]

[a] Department of Chemistry, Payame Noor University, 19395-3697 Tehran, Iran
[b] Department of Chemistry, Faculty of Science, University of Kurdistan, Sanandaj, Iran
[c] Department of Chemistry, Institute for Advanced Studies in Basic Sciences (IASBS), Gavazang, Zanjan, Iran
[d] Institut für Anorganische Chemie, Universität Leipzig, Leipzig, Germany

HIGHLIGHTS

- Three dinuclear complexes based on a Ag^I/β-diketonate/2,3-bis(2-pyridyl)pyrazine ligands.
- Compounds characterized by spectroscopy technical and X-ray crystallography.
- Weak interactions provide additional assembly forces, leading to 3D supramolecular networks.

ARTICLE INFO

Article history:
Received 28 February 2012
Received in revised form 22 April 2012
Accepted 23 April 2012
Available online 1 May 2012

Keywords:
Ag^I
Fluorinated β-diketonate
2,3-Bis(2-pyridyl)pyrazine

ABSTRACT

Three binuclear Ag^I complexes based on a β-diketonate and N-donor ligands, $[Ag_2(2,3\text{-bpp})_2(hfa)_2]$ (**1**), $[Ag_2(2,3\text{-bpp})_2(ftfa)_2]$ (**2**) and $[Ag_2(2,3\text{-bpp})_2(ttfa)_2]$ (**3**), where 2,3-bpp is 2,3-bis(2-pyridyl)pyrazine, Hhfa is hexafluoroacetylacetone, Hftfa is furoyltrifluoroacetone and Httfa is thienoyltrifluoroacetone, were prepared and characterized by elemental analysis, IR and ^1H NMR spectroscopy as well as by X-ray crystallography. Additionally, thermal and electrochemical properties were studied. The complexes are structurally similar to each other. Three nitrogen atoms of the ligand 2,3-bpp in compounds **1**, **2** and **3** act as donors toward two Ag^+ ions in syn-conformation. Abundant weak interactions, such as $\pi\cdots\pi$, C—H···F, C—H···π and C—H···O interactions lead to 3D supramolecular networks for **1**–**3**.

1. Introduction

Supramolecular chemistry and crystal engineering based upon the self-assembly of metal ions and bridging organic ligands have attracted great interest in recent years due to the novel structural topologies and potential applications in optical and magnetic components, catalysis, and electrical conductivity [1–5]. In the past few years, the development of supramolecular chemistry based on coordinative bonds and the hydrogen bonds has provided the possibility to rationally design and prepare supramolecular architectures by noncovalent interactions. It is crucial to meet both geometric and energetic considerations. Lately, a lot of supramolecular assemblies have been achieved by carefully selecting building blocks and organic ligands containing appropriate functional groups through supramolecular interactions (hydrogen bonding, π—π interactions, etc.) [6–12]. The self-assembly of multidentate organic ligands and metal ions has resulted in many beautiful and novel coordination polymeric frameworks. According to former research, designing and synthesizing MOFs (metal organic frameworks) can be influenced by the subtle interplay of many factors such as the geometric preference of metal ions, the sizes and shapes of the organic building blocks, templates, and solvent systems. The high degree of design arises from the coupling of the well understood coordination properties of the individual metal ions and highly developed ligand syntheses within the newer areas of supramolecular chemistry and crystal engineering [13–18]. It is known that fluorinated β-diketonate ligands [19] and 2,3-bis(2-pyridyl)pyrazine [20–22] are good candidates for the construction of coordination frameworks with specific structure due to their N and O donor groups, from which a rich variety of one-, two- and three-dimensional metal–organic polymeric architectures have been constructed. In the synthesis of crystalline materials by design, the assembly of molecular units in predefined arrangements is a key goal. The synthesis of the solid state structures of silver(I) complexes of fluorinated β-diketonate and pyridyl ligands relies on an understanding of their potential C—H···O, C—H···F, C—H···π and π—π intra- and intermolecular interactions [23]. These

* Corresponding author.
E-mail address: f.marandi@gmail.com (F. Marandi).

0022-2860/$ - see front matter © 2012 Elsevier B.V. All rights reserved.
http://dx.doi.org/10.1016/j.molstruc.2012.04.069

non-covalent interactions compete and eventually guide the assembly of the building blocks to form extended solid state low-dimensional architectures [24]. With the aim of constructing coordination architectures, we are interested in using the versatile fluorinated β-diketonates and 2,3-bis(2-pyridyl)pyrazine ligands with silver ion. In this paper, we report the synthesis, crystal structures, thermal gravimetric and cyclic voltammetry properties of $[Ag_2(2,3\text{-bpp})_2(hfa)_2]$ (**1**), $[Ag_2(2,3\text{-bpp})_2(ftfa)_2]$ (**2**) and $[Ag_2(2,3\text{-bpp})_2(ttfa)_2]$ (**3**), where 2,3-bpp is 2,3-bis(2-pyridyl)pyrazine, Hhfa is hexafluoroacetylacetone, Hftfa is furoyltrifluoroacetone and Htttfa is thienoyltrifluoroacetone.

2. Experimental

2.1. Physical measurements

IR spectra were recorded as KBr pellets using a Perkin–Elmer 597 and a Nicolet 510P spectrophotometer. Elemental analyses (C, H, N) were performed using a Carlo ERBA model EA 1108 analyzer. Solution ^{1}H NMR spectra were recorded on a BRUKER DRX-500 AVANCE spectrometer at 500 MHz using d_6-dimethylsulfoxide as solvent. Thermal analyses were carried out on a Seiko Instruments thermal analyzer. Cyclic voltammetry was performed using an Autolab potentiostat/galvanostat 101. The working electrode was a glassy carbon disk (2.0 mm diameter), a Pt wire was used as a counter electrode. The working electrode potentials were measured versus a platinum wire as quasi-reference electrode (all electrodes from Azar Electrode).

2.2. Crystallography

The single crystal X-ray diffraction data of the complexes **1**, **2** and **3** were collected on imaging plate diffractometers IPDS-2T at 180 K (**1**) and IPDS-1 at 213 K (**2**,**3**), respectively, (Stoe & Cie GmbH, Darmstadt, Germany) using Mo-K_α radiation (λ =71.073 pm) [25]. All intensities were corrected for Lorentz and polarization effects. Numerical absorption corrections were applied to all data sets. The structures were solved by direct methods using the program Shelxl-97 and refined by full-matrix least squares based on F^2 using Shelxl-97 [26]. Anisotropic displacement parameters were used for all Ag, C, Cl, F, N, O and S atoms; hydrogen atoms were included in calculated positions. The basic crystallographic data of **1**–**3** are summarized in Table 1. Selected interatomic distances and angles are given in Table 2. Graphical presentations were drawn using Ortep-3 [27].

2.3. Preparation of $[Ag_2(2,3\text{-bpp})_2(hfa)_2]$ (**1**)

A mixture of Ag_2O (116 mg, 0.5 mmol), 2,3-bpp (0.234 g, 1.0 mmol) and Hhfa (208 mg, 1.0 mmol) was stirred in a CH_3CN/H_2O mixture (15 ml, v/v: 1/4). Then, an aqueous NH_3 solution (25%) was poured into the mixture to give a clear solution. The resultant solution was allowed to evaporate slowly in darkness at room temperature for several days to give colorless crystals of **1**. The crystals were washed with a small volume of cold methanol and diethyl ether. m. p., 181 °C Anal. Calc. for $C_{38}H_{22}Ag_2F_{12}N_8O_4$: C, 41.52; H, 2.00; N, 10.20. Found: C, 41.89; H, 2.29; N, 9.94%. IR (KBr, cm^{-1}): 3065 (m), 1615 (s), 1600 (s), 1592 (s), 1530(s), 1518(s), 1460 (s), 1335(m), 1248, 1143, 1025 (m), 770 (m), 650 (w), ^{1}H NMR (DMSO, δ): 8.80 (d, 2H, pyrazine), 8.38 (dd, 2H, pyridyl), 7.89 (m, 2H, pyridyl), 7.70 (dd, 2H, pyridyl), 7.42 (m, 2H, pyridyl), 5.26 (s, 1H, ═CH— of hfa^-).

2.4. Preparation of $[Ag_2(2,3\text{-bpp})_2(ftfa)_2]$ (**2**)

A mixture of Ag_2O (116 mg, 0.5 mmol), 2,3-bpp (0.234 g, 1.0 mmol) and Hftfa (206 mg, 1.0 mmol) was stirred in a CH_3OH/H_2O mixture(15 ml, v/v: 1/1). Then, an aqueous NH_3 solution (25%) was poured into the mixture to give a clear solution. The resultant solution was allowed to evaporate slowly in darkness at room temperature for several days to give colorless crystals of **2**. The crystals were washed with a small volume of cold methanol and diethyl ether. m. p.: 195 °C. Anal. Calc. for $C_{44}H_{28}Ag_2F_6N_8O_6$:

Table 1
Crystal data and structure refinement for **1**–**3**.

	1	**2**	**3**
Identification code	$[Ag_2(2,3\text{-bpp})_2(hfa)_2]$	$[Ag_2(2,3\text{-bpp})_2(ftfa)_2]$	$[Ag_2(2,3\text{-bpp})_2(ttfa)_2]$
Empirical formula	$C_{38}H_{22}Ag_2F_{12}N_8O_4$	$C_{44}H_{28}Ag_2F_6N_8O_6$	$C_{44}H_{28}Ag_2F_6N_8O_4S_2$
Formula weight	1098.38	1094.48	1126.60
Crystal system	Triclinic	Triclinic	Triclinic
Space group	$P\bar{1}$	$P\bar{1}$	$P\bar{1}$
Unit cell dimensions	a = 9.0533(9) Å b = 9.4841(10) Å c = 13.4296(14) Å α = 87.220(8)° β = 89.155(8)° γ = 61.734(7)°	a = 9.2203(7) Å b = 9.4282(6) Å c = 14.0133(10) Å α = 100.740(8)° β = 93.177(9)° γ = 118.321(8)°	a = 9.0789(7) Å b = 9.5637(7) Å c = 14.5576(11) Å α = 96.773(9)° β = 96.236(9)° γ = 116.810(8)°
Volume	1014.36(18) $Å^3$	1038.92(13) $Å^3$	1101.43(14) $Å^3$
Z	1	1	1
Density (calculated)	1.798 g cm^{-3}	1.749 g cm^{-3}	1.698 Mg/m^3
Absorption coefficient	1.072 mm^{-1}	1.030 mm^{-1}	1.063 mm^{-1}
F(000)	540	544	560
θ Range for data collection	2.44–27.90	2.53–27.00	2.43–26.00°
Index ranges	$-11 \leqslant h \leqslant 11$ $-12 \leqslant k \leqslant 12$ $-16 \leqslant l \leqslant 17$	$-11 \leqslant h \leqslant 11$ $-12 \leqslant k \leqslant 12$ $-17 \leqslant l \leqslant 17$	$-10 \leqslant h \leqslant 10$ $-11 \leqslant k \leqslant 11$ $-17 \leqslant l \leqslant 17$
Reflections collected	12,153	10,907	8843
Independent reflections	4811[R(int) = 0.0358]	4225[R(int) = 0.0261]	4039 [R(int) = 0.0243]
Completeness to theta	99.3%	93.2%	93.5%
Data/restraints/parameters	4811/0/290	4225/0/298	4039/0/298
Goodness-of-fit on F^2	1.035	0.902	0.940
$R1$ [$I_0 > 2\sigma(I_0)$]	$R1$ = 0.0263	$R1$ = 0.0245	$R1$ = 0.0378
wR2 (all data)	wR2 = 0.0690	wR2 = 0.0553	wR2 = 0.1156
Largest diff. Peak, hole	0.71, −0.51 e. Å	0.39, −0.28 e. Å	0.96 and −0.83 e. $Å^{-3}$

Table 2
Selected bond lengths/Å and angles/° for **1–3**.

	1	2	3
Ag—N4^{i}	2.270(2)	2.285(2)	2.317(4)
Ag—N2	2.363(2)	2.370(2)	2.379(3)
Ag—N1	2.373(2)	2.394(2)	2.422(3)
Ag—O1	2.484(2)	2.432(1)	2.443(3)
Ag—O2	2.487(1)	2.442(2)	2.457(2)
N4^{i}—Ag—N2	126.05(6)	123.10(6)	121.51(1)
N4^{i}—Ag—N1	129.73(6)	133.20(6)	133.97(1)
N2—Ag—N1	70.01(6)	69.18(6)	69.52(1)
N4^{i}—Ag—O1	109. 73(6)	104.69(7)	107.02(1)
N2—Ag—O1	123.72(6)	131.86(6)	131.10(1)
N1—Ag—O1	81.05(5)	83.19(6)	81.78(1)
N4^{i}—Ag—O2	84.85(6)	86.09(6)	84.92(1)
N2—Ag—O2	103.34(5)	99.49(6)	101.96(1)
N1—Ag—O2	142.55(6)	139.62(6)	139.66(1)
O1—Ag—O2	72.48(6)	76.69(5)	75.22(1)

i: 1 − *X*, 1 − *Y*, 1 − *Z*

C, 48.24; H, 2.56; N, 10.23. Found: C, 48.17; H, 2.79; N, 10.59%. IR (KBr, cm^{-1}): 3070 (m), 1620(s), 1600(s), 1590(m), 1565 (s), 1520 (s), 1473 (s), 1322(m), 1260, 1170, 1125 (m), 1035(m), 1000(m), 780 (m), 640 (w). ^{1}H NMR (DMSO, δ): 8.77 (d, 2H, pyrazine), 8.37(dd, 2H, pyridyl), 7.83–7.89 (m, 3H, pyridyl and furyl), 7.71(dd, 2H, pyridyl), 7.39(m, 2H, pyridyl), 6.96 (d, 1H, furyl), 6.54 (d of d, 1H, furyl), 5.83 (s, 1H, ═CH— of ftfa^{-}).

2.5. Preparation of $[Ag_2(2,3\text{-bpp})_2(ttfa)_2]$ (**3**)

Complex **3** was synthesized in the same way as complex **2** using Httfa (222 mg, 1.0 mmol) in place of Hftfa. m. p.: 171 °C. Anal. Calc. for for $C_{44}H_{28}Ag_2F_6N_8O_4S_2$: C, 46.87; H, 2.48; N, 9.94. Found: C, 47.15; H, 2.29; N, 9.69%. IR (KBr) m (cm^{-1}): 3034(m), 1620(s), 1605(m), 1595(s), 1560 (s), 1500 (s), 1470 (s), 1355(m), 1260, 1210, 1155 (m), 1020(m), 1005(m), 778 (m), 666 (w). ^{1}H NMR (DMSO, δ): 8.78 (d, 2H, pyrazine), 8.34(dd, 2H, pyridyl), 7.60–8.06 (m, 6H, pyridyl), 7.06–7.40 (m, 3H, thenoyl), 5.88 (s, 1H, ═CH— of ttfa^{-}).

3. Result and discussion

3.1. Syntheses, spectroscopic studies, thermogravimetry and cyclic voltammetry

The conventional solution reaction between silver(I) oxide with 2,3-bis(2-pyridyl)pyrazine and derivatives of trifluoromethyldiketonate ligands with 2,3-bis(2-pyridyl)pyrazine in CH_3CN/H_2O or CH_3OH/H_2O mixed solvents yielded crystalline material of $[Ag_2(2,3\text{-bpp})_2(hfa)_2]$ (**1**), $[Ag_2(2,3\text{-bpp})_2(ftfa)_2]$ (**2**) and $[Ag_2(2,3\text{-bpp})_2(ttfa)_2]$ (**3**) (Scheme 1).

The IR spectra of **1**–**3** display the characteristic absorption bands for 2,3-bpp ligands and the β-diketonate anions. The relatively weak absorption bands at around 3065, 3070 and 3034 cm^{-1} are due to the C—H modes involving the aromatic ring hydrogen atoms in **1**, **2** and **3**, respectively. The shift towards higher wave numbers of the characteristic bands of the pyrazine (1592, 1590, 1595 and 1600, 1600, 1605 cm^{-1} in **1**, **2** and **3** versus 1563 and 1580 cm^{-1} in the free ligand) and pyridine (1025, 1035, 1020 cm^{-1} in **1**, **2**, **3** versus 991 cm^{-1} in the free ligand), are indicative of the coordination of the 2,3-bpp molecule [28]. The aromatic ring vibrations of 2,3-bpp in **1**, **2** and **3** in the 1600–1350 cm^{-1} range are somewhat shifted to higher wave-numbers in comparison to the free 2,3-bpp molecule, as expected upon their metal coordination [29]. At the same time, the IR spectra of the complexes show strong bands at 1615, 1620, 1620 cm^{-1} and at 1518, 1515 cm^{-1}, assigned to the ν(C═O) and ν(C═C) (**2**,**3**) stretching of the β-diketonate anions. These bands are at significantly lower energies than those found for free Hhfa, Hftfa, Httfa (1684, 1686, 1676 cm^{-1} assigned to the ν(C═O)) are indicative of β-diketonate chelation to Ag^{I}. The absorption bands in the frequency range 1260–1130 cm^{-1} correspond to the C—F modes of the β-diketonates [30].

The ^{1}H NMR spectra of DMSO solutions of **1**, **2** and **3** display five separated signals for the protons of the 2,3-bpp ligand at 7.4–8.8 ppm and the singlets at 5.26, 5.83 and 5.88 ppm of the

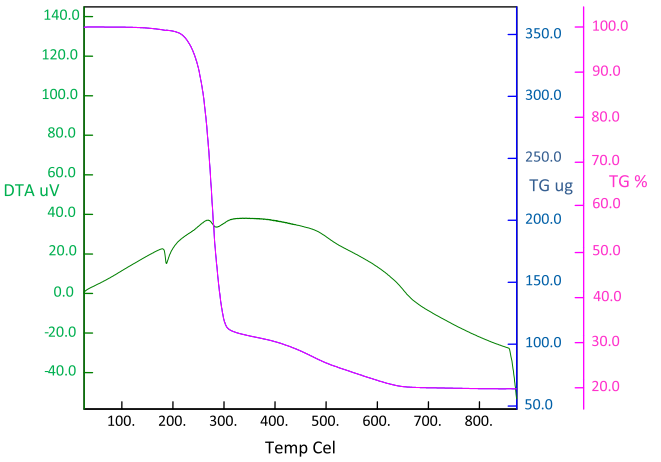

Fig. 1. TG and DTA curves of **1**.

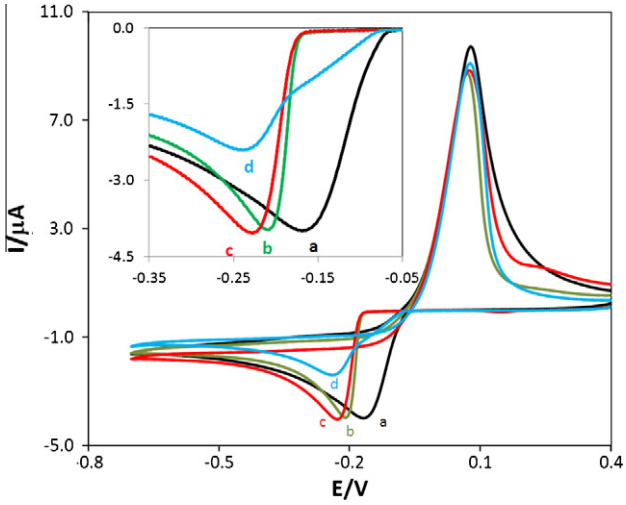

Fig. 2. Cyclic voltammograms of 1.0 mM (a) $AgNO_3$, (b) **3**, (c) **2** and (d) **1** at glassy carbon electrode in DMSO, Supporting electrolyte 0.1 M TBAP and scan rate 100 mVs^{-1}. Inset: expand of catodic peaks.

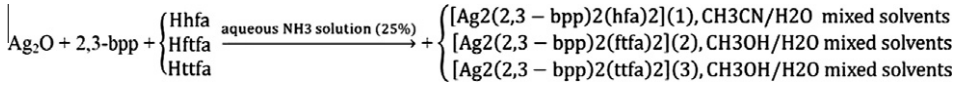

Scheme 1. Syntheses of compounds.

=CH— protons of hfa^-, $ftfa^-$ and $ttfa^-$ anions, respectively. In **2**, three distinct signals of the furyl group appear at 6.54, 6.96 and 7.85 ppm (overlapped with protons of the 2,3-bpp ligand) and in **3**, three distinct signals of thienyl group of the β-diketonate anion appear at 7.06–7.40 ppm.

The TG curves show that complexes **1**, **2** and **3** exhibit similar decomposition pathways, as an example the TG of **1** is shown in Fig. 1. No weight loss is observed up to about 270 °C demonstrating that **1**, **2** and **3** are retained up to these temperatures. The thermal decomposition of the compounds occurs in one step in the temper-

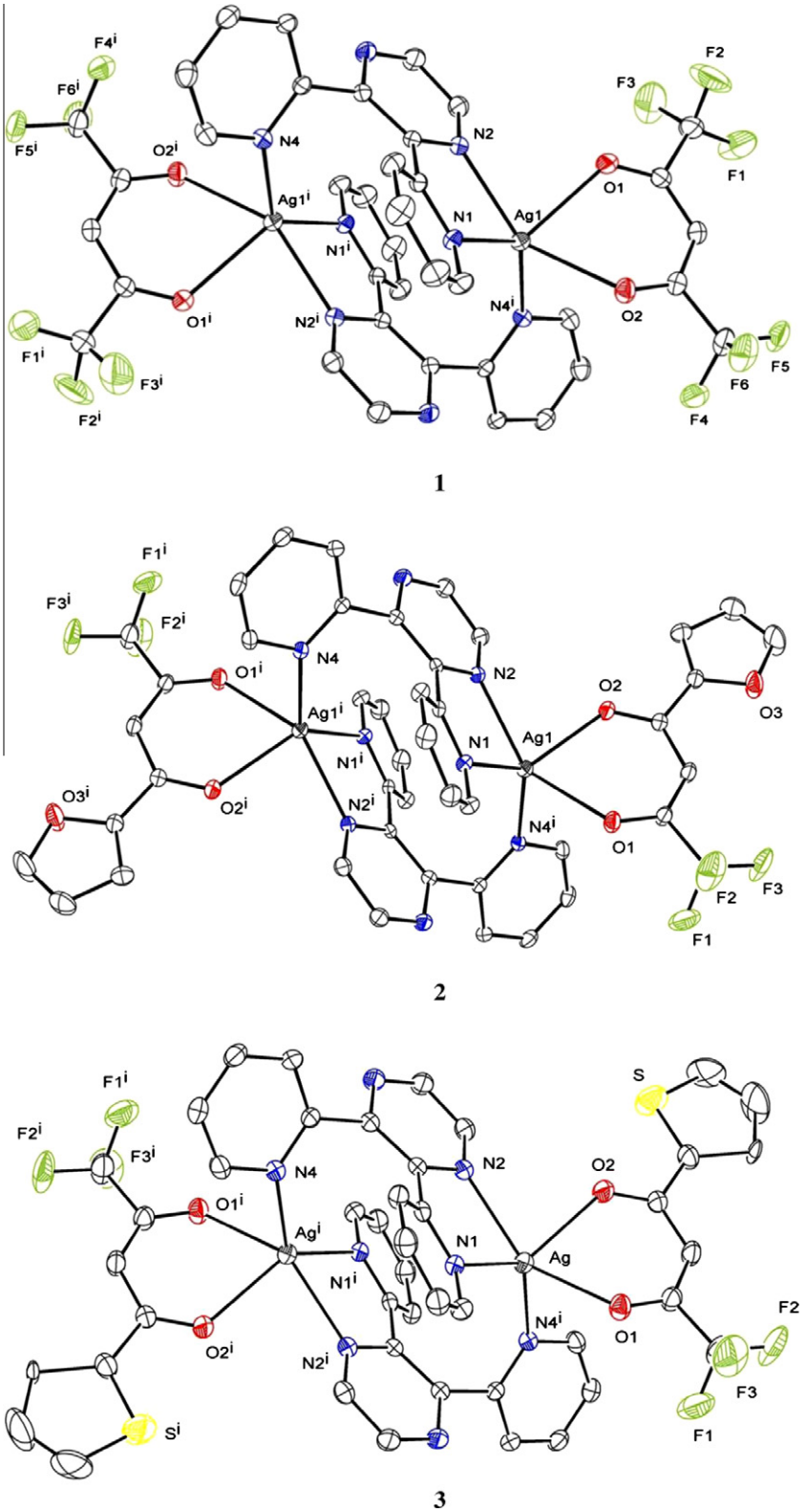

Fig. 3. Ortep view of **1**, **2** and **3**. Displacement ellipsoids are shown at the 40% probability level.

ature range 270–300 °C (almost 80% weight). The mass loss calculations as well as microanalyses of the solid residues suggest that the residue left as a final decomposition product is Ag and the remaining mass of 20.25% for **1** (Calc. 19.66%), 20.80% for **2** (Calc. 19.75%) and 21.00% for **3** (Calc. 19.75%), respectively, is in reasonable agreement well with the expected values.

The electrochemical behavior of the complexes is studied using the cyclic voltammetry in DMSO containing 0.1 M tetrabutylammonium perchlorate. Fig. 2 (curve a) shows the cyclic voltammograms (CVs) of **1**–**3** together with that of $AgNO_3$ under the same conditions. All the cyclic voltammograms exhibit a cathodic peak (C_1) in negative scan and a anodic peak (A_1) in positive scan mode. The cathodic peaks are due to the reduction of the Ag^+ ions, and the anodic peaks are related to the oxidation of Ag produced at the electrode surface. It is clearly shown that the cathodic peak potentials of the complexes shifts to more negative values, −57, −62 and −72 mV for **3**, **2** and **1**, respectively, compared to $AgNO_3$. This indicates the good interaction and more stability of the silver ion in the complex structures [33]. It should be noted that Ag^+ is strongly solvated in DMSO and its interactions are comparable with some cryptands [34]. However, the presence of ligands shifts the cathodic peak potential to more negative values. Additionally, the voltammetric study of the complexes with time shows that they have good kinetic stability.

3.2. Description of the crystal structures of *1*, *2* and *3*

Single crystal X-ray diffraction analysis reveals that the complexes form discrete neutral metallacycles [Ag(2,3-bpp)(β-diketonate)]$_2$, consisting of two 2,3-bpp ligands, two β-diketonate ligands and two Ag^+ ions (Fig. 3), which represents the smallest 2D cyclic assembly possible for closed structures with a 1:1 metal-to-ligand ratio. The two 2,3-bpp ligands are arranged in a face-to-face syn-conformation [31] from opposite directions to coordinate to two Ag^+ ions; each Ag^+ ion is penta-coordinated by three nitrogen atoms (N1, N2 and N4^i) from two different 2,3-dpp ligands and two oxygen atoms (O1 and O2) of one β-diketonate anion (hfa^-, $ftfa^-$ and $ttfa^-$) with the coordination geometry of a distorted bipyramidal geometry (N1 and O2 atoms occupy the axial positions and N2, O1, and N4i define the equatorial sites of the trigonal bipyramid. Ag atom is positioned in a plane formed by N2, O1 and N4i atoms). The Ag—O distances range from 2.432 to 2.487 Å and the Ag—N distances from 2.270 to 2.379 Å (Table 2) [32].

The neutral [Ag(2,3-dpp)(β-diketonate)]$_2$ motif has the center of inversion between the two Ag^+ ions. This leads to the assembly of a typical rectangular cavity enclosed by two ligands and two Ag^+ ions with an Ag···Ag separation of 5.156 Å for **1**, 5.177 Å for **2** and 5.164 Å for **3** as shown in Fig. 2. These distances are shorter than of the reported structures with another β-diketonate (derivatives of benzoyltrifluoroacetonate) ligands [34]. The size of different substitutents ion [34] is larger than in compounds **1**–**3**. It is worth noting that the weak directional intermolecular and π—π stacking interactions have an important role in constructing the supramolecular network of these compounds.

An inspection of the data of **1**, **2** and **3** for weak directional intermolecular interactions by the programs PLATON and MERCURY [35], which were used for calculating the supramolecular interactions, has shown that there are O···H—C, F···H—C, F···S, F···π, and F···F interactions [19] (Table 3). In addition, there are relatively strong C—H···π interactions (Fig. 4, Table 3) within this class of weak non-covalent contacts [36]. The packing diagram of **1** (Fig. 5) exhibits a 2D self-assembled structure through π···π stacking (slipped face-to-face), with 3.457 Å distance between the pyridine rings, remarkably shorter than for normal π···π stacking [37]. In addition to π···π stacking, in **2**, and **3**, 3D supramolecular networks are constructed by O···H—C and F···H—C interactions that are substantially shorter than the van der Waals distances of 2.77 Å for the O···H and 2.67 Å for the F···H distance [38] (Table 3, Fig. 6).

A useful comparison to **1**, **2** and **3** is provided by a recent structural study of the dinuclear complexes of Ag^+ with nitrate as anion [31]. Average Ag—N distances in **1**, **2** and **3** are longer than in [Ag(2,3-bpp)(NO_3)]$_2$, and two aryl ring planes of 2,3-bpp (plane of pyridyl and pyrazine) form angles of 57.73, 57.76 and 52.34° for **1**, **2**, **3**, respectively, that is more than for [Ag(2,3-bpp)(NO_3)]$_2$ (47.53°). It seems reasonable to assume that differences in the

Table 3
Intermolecular interactions for **1**–**3**.

	A···H (Å)	A···B (Å)	A···H—B (°)
1			
O2···H3—C3 (−*X*, 1−*Y*,1− *Z*)	2.506	3.323	144.12
O1···H12—C12 (−*X*, 2 − *Y*, 1 − *Z*)	2.456	3.382	164.53
O2···H8—C8 (*X*, −1 + *Y*, *Z*)	2.549	3.479	166.00
F5···H13—C13 (*X*, −1 + *Y*, 1 + *Z*)	2.569	3.137	118.67
F3···H14—C14 (*X*, *Y*, 1 + *Z*)	2.626	3.375	136.11
F5···F5 (1 − *X*, −*Y*, 2 − *Z*)	–	2.894	–
π—π stacking (slipped face-to-face)	–	3.542	–
H11···Cg (C6···N2)(−*X*, 2 − *Y*, 1 − *Z*)	–	2.703	–
2			
O2···H12—C12 (1 − *X*, −*Y*,1 − *Z*)	2.515	3.449	172.11
O1···H3—C3 (2 − *X*, 1 − *Y*, 1 − *Z*)	2.471	3.330	152.04
O1···H8—C8 (1 + *X*, 1 + *Y*, *Z*)	2.697	3.621	167.60
F1···H9—C9 (1 + *X*, 1 + *Y*, *Z*)	2.649	3.281	125.10
F3···H14—C14 (1 + *X*, 1 + *Y*, 1 + *Z*)	2.607	3.327	133.72
F2···π (C13···C14)(2 − *X*, 1 − *Y*,1 − *Z*)	–	3.176	–
π—π stacking (slipped face-to-face)	–	3.457	–
H11···Cg (N2···C6)(1 − *X*, −*Y*, 1 − *Z*)	–	2.714	–
3			
O2···H12—C12 (1 − *X*, −*Y*, 1 − *Z*)	2.561	3.492	170.97
O1···H3—C3 (2 − *X*, 1 − *Y*, 1 − *Z*)	2.376	3.251	154.84
N2···H11—C11 (1 − *X*, −*Y*, 1 − *Z*)	2.851	3.509	128.07
F2···S (1 + *X*, 1 + *Y*, *Z*)	–	3.259	–
π—π stacking (slipped face-to-face)	–	3.443	–
H11···Cg(N2···C6)(1 − *X*, −*Y*, 1 − *Z*)	–	2.772	–

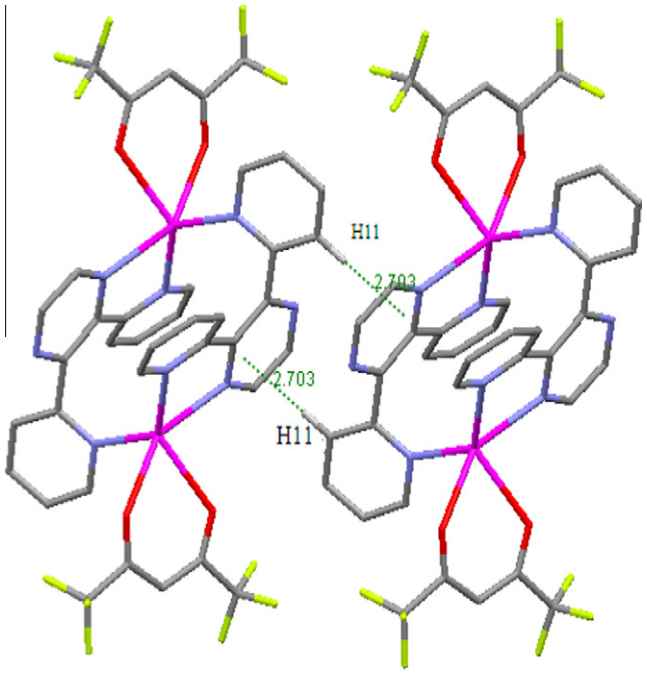

Fig. 4. Packing diagram of **1**, view along [100], showing C—H···π interactions.

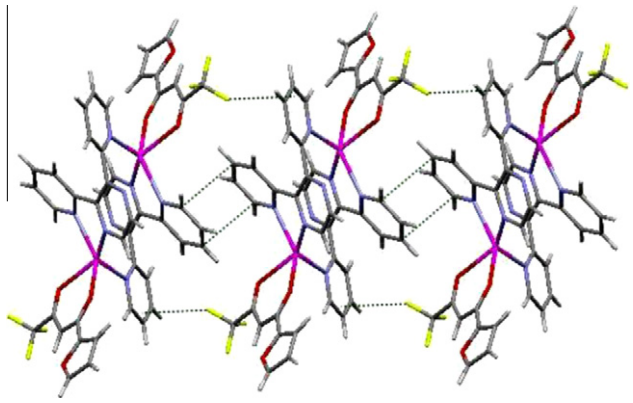

Fig. 5. A part of the two-dimensional network of **2** view along [010] plane, generated from F···π and π···π stacking interactions.

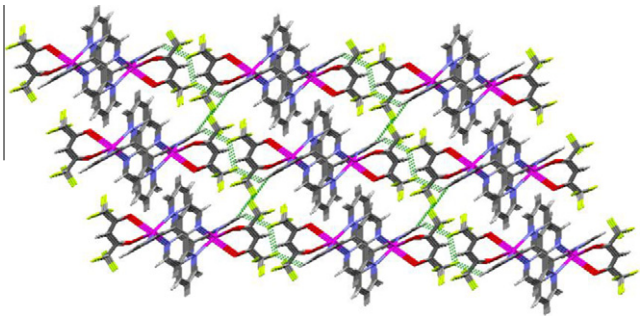

Fig. 6. A part of three-dimensional network of **1** view along [010], generated from intermolecular interactions (Table 3).

dihedral angles between the aryl ring planes of 2,3-bpp coordinating to Ag^+ are influenced the network of directed intermolecular interactions and the coordination of the anions.

4. Conclusion

In summary, we have successfully prepared three new binuclear complexes based on 2,3-bis(2-pyridyl)pyrazine, fluorinated β-diketonate ligands and silver ions. The complexes are structurally similar to each other. The three nitrogen atoms of the 2,3-bpp ligand in all three compounds act as donors toward two Ag^+ ions in syn-conformation. Abundant weak interactions, such as π···π, F···π, C—H···F, C—H···O and F···F interactions between ligands of binuclear complexes, provide additional assembly forces, leading to 3D supramolecular networks for **1**–**3**.

Supporting information

Full cif depositions, excluding structure factor amplitudes, reside with the Cambridge Crystallography Data center, CCDC-869063–869065 for **1**, **2** and **3**. Copies of the data can be obtained, free of charge, on application from CCDC, 12 Union Road, Cambridge CB2 1EZ, UK (fax: +44 1223 336033 or e-mail: deposit@ccdc.cam.ac.uk).

Acknowledgment

Support of this investigation by Payame Noor University is gratefully acknowledged by F.M.

References

[1] A.J. Blake, S.J. Hill, P. Hubberstey, W.-S. Li, J. Chem. Soc. Dalton Trans. (1997) 913.
[2] A.J. Blake, N.R. Champness, P. Hubberstey, W.-S. Li, M.A. Withersby, M. Schröder, Coord. Chem. Rev. 183 (1999) 117.
[3] A.J. Blake, N.R. Champness, P.A. Cooke, J.E.B. Nicolson, C. Wilson, J. Chem. Soc. Dalton Trans. (2000) 3811.
[4] O.M. Yaghi, M. O'Keeffe, N.W. Ockwig, H.K. Chae, M. Eddaoudi, J. Kim, Nature 423 (2003) 705.
[5] S. Kitagawa, R. Kitaura, S. Noro, Angew. Chem. 116 (2004) 2388; Angew. Chem. Int. Ed. 43 (2004) 2334.
[6] J.M. Lehn, Supramolecular Chemistry, VCH, Weinheim, 1995.
[7] D.F. Sun, R. Cao, Y.Q. Sun, W.H. Bi, X.J. Li, Y.Q. Wang, Q. Shi, X. Li, Inorg. Chem. 42 (2003) 7512.
[8] B.B. Ding, Y.Q. Weng, Z.W. Mao, C.K. Lam, X.M. Chen, B.H. Ye, Inorg. Chem. 44 (2005) 8836.
[9] X.L. Wang, C. Qin, E.B. Wang, Cryst. Growth Des. 6 (2006) 439.
[10] A.K. Ghosh, D. Ghoshal, E. Zangrando, Polyhedron 26 (2007) 4195.
[11] N.L.S. Yue, M.C. Jennings, R.J. Puddephatta, Eur. J. Inorg. Chem. 12 (2007) 1690.
[12] W.Z. Lee, Y.L. Kang, T.L. Wang, C.C. Su, T.S. Kuo, Cryst. Growth Des. 8 (2008) 2614.
[13] M. Eddaoudi, D.B. Moler, H. Li, B. Chen, T.M. Reineke, M. O'Keeffe, O.M. Yaghi, Acc. Chem. Res. 34 (2001) 319.
[14] A.J. Blake, G. Baum, N.R. Champness, S.S.M. Chung, P.A. Cooke, D. Fenske, A.N. Khlobystov, D.A. Lemenovskii, W.-S. Li, M. Schröder, J. Chem. Soc. Dalton Trans. (2000) 4285.
[15] A.J. Blake, N.R. Champness, M. Crew, S. Parsons, New J. Chem. (1999) 13.
[16] R. Robson, J. Chem. Soc., Dalton Trans. (2000) 3735.
[17] O.M. Yaghi, H. Li, J. Am. Chem. Soc. 118 (1996) 295.
[18] M.-L. Tong, X.-M. Chen, S.W. Ng, Inorg. Chem. Commun. (2000) 436.
[19] (a) F. Marandi, Z. Nikpey, M. Khosravi, H.-K. Fun, M. Hemamalini, J. Coord. Chem. 64 (2011) 3012;
(b) F. Marandi, A. Morsali, Inorg. Chim. Acta 370 (2011) 526;
(c) F. Marandi, R. Rutvand, M. Rafiee, J.H. Goh, H.-K. Fun, Inorg. Chim. Acta 363 (2010) 4000;
(d) F. Marandi, Z. Nikpey, J.H. Goh, H.-K. Fun. Z. Naturforsch. 65b (2010) 128;
(e) F. Marandi, H. Krautscheid, Z. Naturforsch. 64b (2009) 1027;
(f) F. Marandi, S. Chantrapromma, H.-K. Fun, J. Coord. Chem. 62 (2009) 249;
(g) H. Ahmadzadi, F. Marandi, A. Morsali, J. Organomet. Chem. 694 (2009) 3565;
(h) F. Marandi, M. Khosravi, H.-K. Fun, Z. Anorg, Allg. Chem. 634 (2008) 2617;
(i) F. Marandi, H.-K. Fun, Z. Anorg, Allg. Chem. 634 (2008) 1123;
(j) F. Marandi, A. Aslani, A. Morsali, J. Coord. Chem. 61 (2008) 882;
(k) F. Marandi, A. Morsali, A.A. Soudi, Z. Anorg, Allg. Chem. 633 (2007) 661;
(l) F. Marandi, N. Asghari, M. Ghorbanloo, A.A. Soudi, P. Mayer, Z. Anorg, Allg. Chem. 633 (2007) 536;
(m) J.M. Harrowfield, F. Marandi, A.A. Soudi, Inorg. Chim. Acta 358 (2005) 4099;
(n) J.M. Harrowfield, S. Maghaminia, A.A. Soudi, Inorg. Chem. 43 (2004) 1810.
[20] (a) R.R. Ruminski, K.D.K. Zimmer, K.A. Rita, M.A. Knobbe, C. Dean, Inorg. Chim. Acta 362 (2009) 1772;
(b) F.S. Delgado, F. Lahoz, F. Lloret, M. Julve, C. Ruiz-Perez, Cryst. Growth Des. 8 (2008) 3219.
[21] (a) K. Ha, Acta Crystallogr. Sect. E: Struct. Rep. Online 67m (2011) 1454;
(b) A. Jain, C. Slebodnick, B.S.J. Winkel, K.J. Brewer, J. Inorg. Biochem. 102 (2008) 1854;
(c) S.M. Arachchige, K.J. Brewer, Inorg. Chem. Commun. 10 (2007) 1159;
(d) F. Kennedy, N.M. Shavaleev, T. Koullourou, Z.R. Bell, J.C. Jeffery, S. Faulkner, M.D. Ward, Dalton Trans. (2007) 1492;
(e) J.M.D. Zapiter, B.M. Tissue, K.J. Brewer, J. Coord. Chem. 64 (2011) 3366;
(f) Q. Gao, Y.-B. Xie, S. Chen, D. Wang, J. Chem. Crystallogr. 37 (2007) 797;
(g) M. Newell, J.A. Thomas, Dalton Trans. (2006) 705.
[22] L. Cunha-Silva, R. Ahmad, M.J. Carr, A. Franken, J.D. Kennedy, M.J. Hardie, Cryst. Growth Des. 7 (2007) 658.
[23] F. Marandi, M. Ghadermazi, A. Marandi, I. Pantenburg, G. Meyer, J. Mol. Struct. 1006 (2011) 136.
[24] (a) C.B. Aakeroy, A.M. Beatty, B.A. Helfrich, Angew. Chem. Int. Ed. 40 (2001) 3240;
(b) C.B. Aakeroy, A.M. Beatty, D.S. Leinen, Cryst. Growth Des. 1 (2001) 47;
(c) C.B. Aakeroy, A.M. Beatty, D.S. Leinen, Cryst. Eng. Commun. 2 (2000) 145.
[25] X-AREA, Stoe & Cie Darmstadt, Germany, 2006.
[26] G.M. Sheldrick, Acta Cryst. A64 (2008) 112.
[27] L.J. Farrugia, J. Appl. Crystallogr. 30 (1997) 565.
[28] H.D. Stidham, J.V. Tucci, Spectrochim. Acta A 23 (1962) 2233.
[29] J. Carranza, H. Grove, J. Sletten, F. Lloret, M. Julve, P.E. Kruger, C. Eller, D.P. Rillema, Eur. J. Inorg. Chem. (2004) 4836.
[30] S. Bureekaew, S. Horike, M. Higuchi, M. Mizuno, T. Kawamura, D. Tanaka, N. Yanai, S. Kitagawa, Nat. Mater. 8 (2009) 831.
[31] Z.-Y. Zhou, Y. Cai, H.-C. Fang, Q.-G. Zhan, H.-J. Jin, Y.-H. Feng, Y.-P. Cai, Inorg. Chim. Acta 363 (2010) 877.

[32] I.M. Kolthoff, E.B. Sandel, E.J. Meehan, S. Brukenestein, Quantitative Chemical Analysis, fourth ed., Macmillan, London, 1971.
[33] K. Izutsu, Electrochemistry in Nonaqueous Solutions, Wiley-VCH Verlag GmbH& Co. KGaA, 2002.
[34] F. Marandi, A. Marandi, M. Ghadermazi, H. Krautscheid, M. Rafiee, J. Coord. Chem. 65 (2012) 1882.
[35] MERCURY 1.4.1, Copyright Cambridge Crystallographic Data Centre, 12 Union Road, Cambridge, CB2 1EZ, UK, (2001–2005).
[36] F. Marandi, H.-K. Fun, C. Chantrapromma, J. Coord. Chem. 62 (2009) 2155.
[37] L. Saghatforoush, F. Marandi, I. Pantenburg, G. Meyer, Z. Anorg, Allg. Chem. 635 (2009) 1523.
[38] (a) G. Althoff, J. Ruiz, V. Rodriguez, G. Lopez, J. Perez, C. Janiak, Cryst. Eng. Commun 8 (2006) 662;
(b) J. Emsley, The Elements, Oxford University Press, Oxford, 1989.